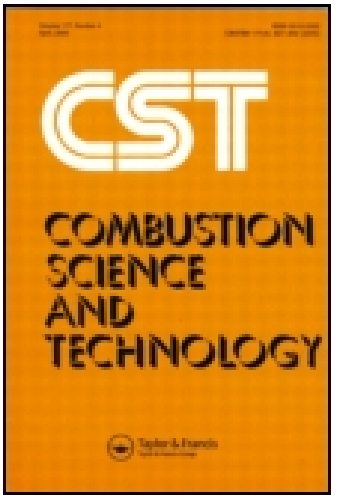

Combustion Science and Technology
Publication details, including instructions for authors and subscription information:
http://www.tandfonline.com/loi/gcst20

Calibration of a Knock Prediction Model for the Combustion of Gasoline-LPG Mixtures in Spark Ignition Engines

Stefano Beccari[a], Emiliano Pipitone[a] & Giuseppe Genchi[a]
[a] Department of Chemical, Management, Information and Mechanical Engineering, University of Palermo, Palermo, Italy
Accepted author version posted online: 09 Sep 2014.Published online: 21 Jan 2015.

Combust. Sci. Technol., 187: 721–738, 2015

ISSN: 0010-2202 print / 1563-521X online
DOI: 10.1080/00102202.2014.960925

Taylor & Francis
Taylor & Francis Group

CALIBRATION OF A KNOCK PREDICTION MODEL FOR THE COMBUSTION OF GASOLINE-LPG MIXTURES IN SPARK IGNITION ENGINES

Stefano Beccari, Emiliano Pipitone, and Giuseppe Genchi
Department of Chemical, Management, Information and Mechanical Engineering, University of Palermo, Palermo, Italy

Gaseous fuels, such as liquefied petroleum gas (LPG) and natural gas (NG), thanks to their good mixing capabilities, allow complete and cleaner combustion than gasoline in spark ignition (SI) engines, resulting in lower pollutant emissions and particulate matter. In a previous work the authors showed that the simultaneous combustion of gasoline and LPG improves an SI engine efficiency with respect to pure gasoline operation with any significant power loss. The addition of LPG to the gasoline-air mixture produces an increase in knock resistance that allows running the engine at full load with overall stoichiometric mixture and better spark advance. In order to predict both performance and efficiency of engines fed by LPG-gasoline mixtures, a specific combustion model and in particular a knock prediction sub-model is required. Due to the lack of literature works about this matter, the authors investigated the knock resistance of LPG-gasoline mixtures. As a result, a reliable knock prediction sub-model has been obtained. The model can be easily implemented in thermodynamic simulations for a knock-safe engine performance optimization. The authors recorded light knocking in-cylinder pressure cycles on a cooperative fuel research (CFR) engine fueled by LPG-gasoline mixtures in different proportions. The tests were performed varying the compression ratio, the spark advance, and the inlet mixture temperature. The collected data have been used to calibrate and then compare two classical knock-prediction models. The models have been calibrated with a heterogeneous set of experimental data in order to predict knock occurrence in SI engines of different kinds. The results show that the models predict the knock onset position with a maximum error of around 6 crank angle degrees (CAD).

Keywords: Knocking; Liquefied petroleum gas; Spark ignition engine

INTRODUCTION

In the last decades many automotive industries focused their research effort on alternative fuels. As regards spark ignition (SI) engines, the gaseous fuels, such as liquefied petroleum gas (LPG) and natural gas (NG), proved to be valid alternatives to gasoline. Thanks to higher knocking resistance gaseous fuels allow the engine to run, even at full

Received 12 March 2014; revised 31 July 2014; accepted 29 August 2014.

Address correspondence to Stefano Beccari, Department of Chemical, Management, Information and Mechanical Engineering, University of Palermo, viale delle Scienze, edificio 8, Palermo 90128, Italy. E-mail: stefano.beccari@unipa.it

Color versions of one or more of the figures in the article can be found online at www.tandfonline.com/gcst.

load, with stoichiometric fuel mixture and optimal spark advance thus increasing engine efficiency and reducing pollutant emissions. The gasoline operated engine instead requires, at high loads, a rich mixture to avoid knocking occurrence. The automotive market proposes nowadays a wide variety of bi-fuel engines that may be fed either with gasoline or with a gaseous fuel (NG or LPG). These engines are usually designed for gasoline operation; hence, they do not fully exploit the higher knocking resistance of gaseous fuel, which would allow higher engine compression ratios and then higher thermodynamic efficiency. In previous works, Pipitone and Beccari (2009a, 2010) showed that the simultaneous combustion of gasoline and NG or gasoline and LPG in a SI engine allows to obtain the low specific fuel consumption and pollutant emissions of gaseous fuel together with nearly the high performance of gasoline. This innovative combustion process was called by the authors "Double-Fuel" to differentiate it from both bi-fuel and Dual Fuel mode. The Double Fuel combustion can be considered as a third operation mode of bi-fuel engines, which are normally run either with gasoline or with gas, and is quite different from the Dual Fuel combustion, in which the autoignition of a small quantity of one of the two fuels is used to ignite and start the combustion of a second fuel (usually gaseous). In Double Fuel combustion, instead, the spark triggers ignition and the two fuels, homogeneously mixed with air, burn simultaneously through the same flame front. Double Fuel operation can be implemented in current production "bi-fuel" engines simply programming the electronic control unit; in particular, the double fuel injection timing and spark advance maps should be added by means of a calibration process. A huge amount of experimental tests must be carried out in order to obtain accurate injection and spark timing maps. Computer simulations represent a fundamental step for design and performance optimization; engine models give a valid first indication for fuel injection time and spark advance allowing a reduction in the amount of experimental tests to be carried out. However, since knocking is a crucial issue concerning SI engines, a reliable auto-ignition sub-model valid for double-fuel operation should be employed so as to safely maximize engine efficiency. The auto-ignition sub-model should estimate the knock onset with acceptable accuracy for each proportion between the two fuels (natural-gas and gasoline or LPG and gasoline). The knock occurrence prediction sub-models most encountered in the literature can be grouped in two main categories: ignition delay models and detailed chemical kinetic models. Ignition delay models base their prediction on the unburned gas pressure and temperature history and usually need some experimental data for calibration (Boehman, and Le Corre, 2008; Douaud and Eyzat, 1978; Lämmle, 2005; Linvengood and Wu, 1955; Pipitone and Beccari, 2009b; Soylu and Gerpen, 2003; Wayne et al., 1998). Instead, detailed chemical kinetic models take into account the elementary reaction steps that occur during the combustion process (Moses et al., 1995; Westbrook and Pitz, 1990). Unfortunately, due to fuel's complexity, some of the elementary reactions may be unknown; moreover, due to the high number of reactions to consider, chemical kinetic sub-models always require a great computational effort. For these reasons, the first category is often preferred for the estimation of unburned gas auto-ignition time. The models based on ignition delay originate from experiments with rapid compression machines (Linvengood and Wu, 1955) in which the pressure and temperature of a fuel-air mixture is rapidly increased and then kept constant until auto-ignition occurs. The ignition delay τ, defined as the time between the end of pressure increase and auto-ignition, can be correlated with the constant pressure p and temperature T by means of an Arrhenius type equation:

$$\tau_{[\mathrm{sec}]} = A \cdot p_{[\mathrm{bar}]}^{-n} \cdot e^{E/R \cdot T\,[\mathrm{K}]} \tag{1}$$

where E (J/mol) is the fuel activation energy, R (J/mol K) is the universal gas constant, while A and n are fuel dependent constants, which can be tuned by means of experimental data. Since in SI engines the unburned gas pressure and temperature are far from being constant, the above correlation is employed with two different approaches: the Livengood and Wu integral approach (Douaud and Eyzat, 1978; Heywood, 1988; Lämmle, 2005; Linvengood and Wu, 1955; Pipitone and Beccari, 2009b; Ramos, 1989; Soylu and Gerpen, 2003; Wayne et al., 1998) and the ignition delay approach (Boehman, and Le Corre, 2008). The first is based on the evaluation of the following knock integral (KI):

$$KI(t) = \int_{t_{IVC}}^{t} \frac{dt}{\tau} = \int_{t_{IVC}}^{t} \frac{dt}{A \cdot p^{-n} \cdot e^{B/T}} \tag{2}$$

where t_{IVC} is the inlet valve closure time, while the constant B substitutes the ratio E/R. According to this method, the knock onset time t_{KO} is obtained when the integral reaches the value of 1:

$$KI(t_{KO}) = \int_{t_{IVC}}^{t_{KO}} \frac{dt}{A \cdot p^{-n} \cdot e^{B/T}} = 1 \tag{3}$$

This condition corresponds to a critical concentration of the intermediate combustion products needed for auto-ignition. Instead, the second method evaluates the ignition delay (ID), with respect to spark time, by means of the unburned gas mean pressure p_m and temperature T_m (estimated during the combustion period):

$$ID = A \cdot p_m^{-n} \cdot e^{B/T_m} \tag{4}$$

The purpose of the present work was to provide a knock prediction sub-model to be used in engine thermodynamic simulations for a knock-safe performance optimization of engines fueled by LPG-gasoline mixtures in different proportions. This has been fulfilled following both the knock-integral method of Eqs. (2) and (3) and the ID method of Eq. (4), whose constants have been tuned by means of experimental data collected on a cooperative fuel research (CFR) engine. The two methods have been compared in terms of knock prediction accuracy. The authors calibrated the models by means of a heterogeneous set of pressure and temperature histories. The CFR engine allows to significantly differentiate pressure and temperature histories by changing volumetric compression ratio, spark advance, and inlet mixture temperature. In the performed tests, the compression ratio and spark advance variation produced an increase of maximum combustion pressure from 23 to 32 bar for gasoline and from 28 to 38 bar for LPG (being the fuel dependent increment around 20%). The models have been calibrated with a heterogeneous set of pressure and temperature histories in order to predict knock occurrence in SI engines of different kinds (aspirated or supercharged), different geometries (compression ratio), fueled with LPG-gasoline mixtures in different proportions. The calibrated models can be easily implemented in numerical simulations involving the same fuel mixture and different engines since the tuned constants depend only on fuel type while all SI engines provide similar pressure and temperature histories of the unburned gas (Douaud and Eyzat, 1978).

EXPERIMENTAL TESTS AND RESULTS

The experimental campaign of the present work has been carried out using a CFR engine (ASTM International, 2013) manufactured by Dresser Waukesha (see Table 1 for main engine specifications).

The CFR is a four-stroke two-valve stationary single-cylinder spark-ignition engine. The particular engine arrangement allows compression ratio (CR) to vary quickly and accurately from 4.5 to 16 by moving the engine head (fixed to the cylinder sleeve) with respect to the piston. The combustion chamber is of discoid type and its basic configuration does not change with the compression ratio (Figure 1). The CFR engine is connected to an electric synchronous motor that keeps a constant speed of 900 rpm both in fired and

Table 1 CFR engine specifications

Manufacturer	Dresser Waukesha
Model	F1/F2 octane
Compression ratio	4.5:16
Bore	82.6 mm
Stroke	114.3 mm
Connecting rod length	254.0 mm
Displacement	611.2 cm^3
Speed	900 rpm

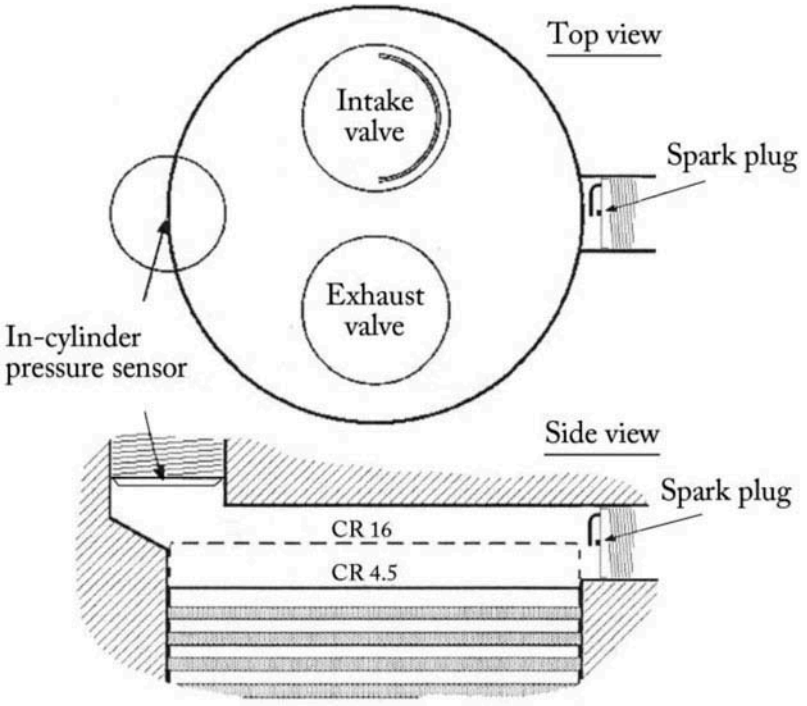

Figure 1 CFR engine combustion chamber with the in-cylinder piezoelectric pressure sensor.

motored condition. The engine is equipped with an electronically controlled inductive discharge ignition system and with two electric heaters, which have been connected to two independent PID control systems (Omega CN4116) in order to maintain both inlet air temperature and air/fuel mixture temperature at the required values during the tests. All of the temperatures were measured using K-type thermocouples.

As regards fuel supply, a standard CFR engine features an original carburettor system, which does not allow the use of gaseous fuels. Hence, the authors endowed the CFR engine with two independent injection systems in order to feed it with either gasoline or LPG and to accurately control the air-fuel ratio. Two port fuel injectors were placed on the CFR intake duct (Figures 2 and 3), before the carburettor that was not used in the tests.

As shown in Figure 2, the gaseous fuel, stored in a tank, flows through a Bronkhorst mini CORI-FLOW® Coriolis effect mass flow meter (with $0.1 \div 2$ kg/h range of measurement and accuracy of $\pm 0.2\%$ of reading) and then through a pressure regulator used to keep the injector feed pressure at 3 bar. The gaseous fuel is injected by means of a Bosch injector.

As also shown in Figure 2, the gasoline injection system is composed of an electric fuel pump, an automatic pressure regulator used to maintain a constant injection pressure of 4 bar, and a Bosch gasoline port injector. During the tests, the gasoline mass flow was evaluated on the basis of the imposed injection time by means of a proper injector flow chart previously experimentally determined. A personal computer was used to manage the two injection systems and perform data acquisition, by means of an expressly designed software developed by the authors in LabVIEW environment. Figure 4 schematically represents the electrical circuit employed for the activation of each fuel injector, mainly composed by the

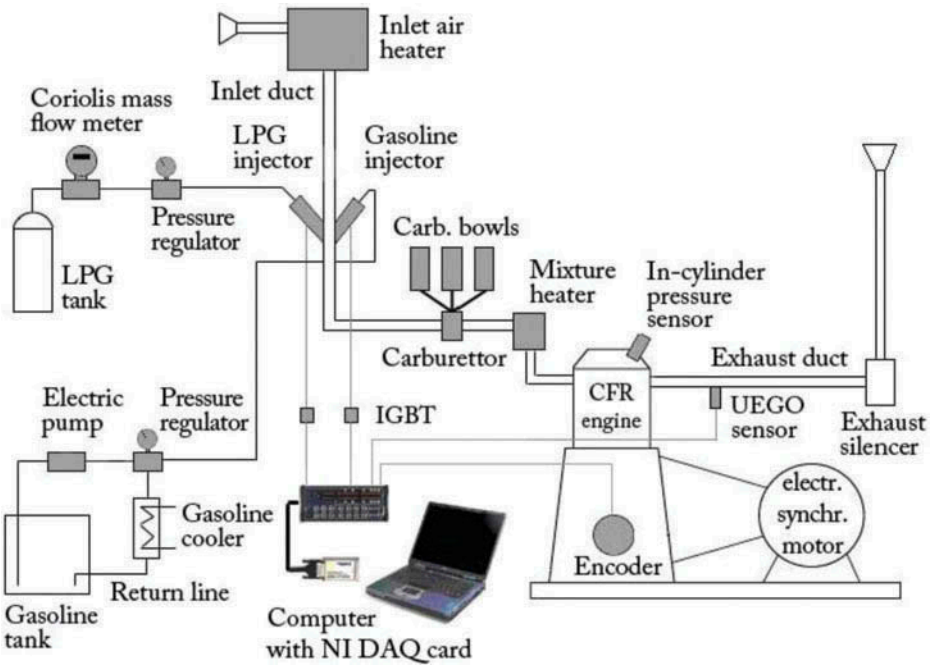

Figure 2 Experimental system layout.

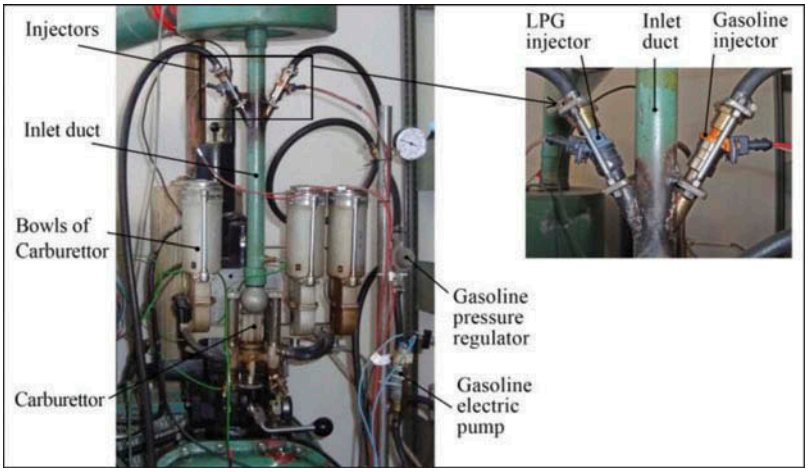

Figure 3 Fuel supply systems: carburettor, LPG injector, and gasoline injectors.

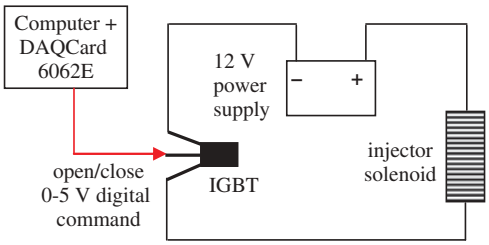

Figure 4 Injector control system.

power supply, the injector solenoid, and an IGBT transistor, which acts as a digital switch, thus opening or closing the electrical circuit based on the voltage level at its input (0 and 5 Volt, respectively).

A National Instruments DAQCard 6062E programmed in LabVIEW environment has been used to generate the necessary 0–5 V digital pulses for the IGBT, whose high level (5V) duration is exactly the injection time: the modulation of this high level width allowed hence the precise control of the amount of fuel injected. A closed-loop control, using as feedback the output signal of a universal exhaust gas oxygen (UEGO) sensor placed in the exhaust duct, allowed to obtain a stoichiometric air-fuel ratio. The output of the UEGO sensor has been corrected by means of proper coefficients in order to take into account the variation of the mixture H/C ratio with the LPG fraction: for each fuel mixture tested, the H/C ratio has been calculated on the basis of the measured fuel mass flow rates. All of the relevant quantities (intake duct pressure, exhaust gas oxygen concentration, LPG mass flow, inlet air, and air-fuel mixture temperatures) were acquired by means of the mentioned National Instruments DAQCard 6062E using as trigger the pulse generated by an incremental optical encoder connected to the engine crankshaft. The same trigger has been employed to synchronize the injection digital pulse with the piston movement. Knock occurrence was monitored using a Kistler piezoelectric pressure sensor, flush mounted on the combustion chamber (Figure 1). A second personal computer was used to process the

in-cylinder pressure signal that was acquired at 120 kHz sampling frequency by means of a National Instruments DAQCard 6062E and using the encoder single pulse per revolution to trigger the acquisition (Figure 2). The manifold absolute pressure (MAP) was measured by means of a DRUCK piezoresistive pressure sensor and has been used to compensate the acquired pressure cycles (Brunt and Pond, 1997; Randolph, 1990). A fundamental aspect in indicating analysis is the precise determination of the top dead center (TDC) position (Pipitone, 2008; Pipitone et al., 2008) which has been accomplished by the use of a Kistler capacitive sensor 2629B, characterized by a 0.1 crank angle degrees (CAD) accuracy.

In order to differentiate as much as possible the unburned gas pressure and temperature histories, the experimental campaign has been designed fixing, for each operative condition, the spark advance and the inlet mixture temperature and increasing the engine CR until light knocking occurrence; this has been made for two different spark advances, namely, 10 CAD and 30 CAD before TDC, and four different inlet mixture temperatures, namely, 50°C, 80°C, 110°C, and 140°C; the spark advances have been fixed to avoid combustion ignition onset too different from that of actual engines. Five fuel mixtures composed by LPG and gasoline in different proportions, where tested, as reported in Table 2: here LPG mass fraction represents the ratio between LPG mass and total fuel mass in the mixture. The overall air-fuel ratio was kept stoichiometric. For each of the 40 operative conditions tested (resumed in Table 2) 50 knocking cycles were sampled. The model has been calibrated by means of so many different pressure and temperature histories in order to predict knocking occurrence in engines of different kinds (i.e., aspirated and supercharged) and geometries (i.e., compression ratio). Table 3 resumes the compression ratios used in all of the operative conditions tested.

The characteristics of gasoline and commercial LPG used in the tests are reported in Table 4.

The unburned mixture temperature T was calculated, from inlet valve closure (IVC) to spark ignition (SI) time, by means of the perfect gas law:

$$T = T_{IVC} \frac{p \cdot V}{p_{IVC} \cdot V_{IVC}} \tag{5}$$

where V is the in-cylinder volume, p is the gas pressure, p_{IVC}, V_{IVC}, and T_{IVC} are the pressure, volume, and temperature at IVC. The mixture temperature T_{IVC} has been considered equal to the inlet mixture temperature T_{MAN} neglecting, in this way, the cylinder walls heat transfer. From the start of combustion the burned and unburned gas temperatures are different and the corresponding masses change continuously so Eq. (5) cannot be used. After

Table 2 Test conditions

Engine speed	900 rpm
Pre-heated air temperature	38 ± 2.8°C
Air/fuel mixture inlet temperature (T_{MAN})	50°C, 80°C, 110°C, 140°C
Engine load condition	Full load
Compression ratio (CR)	Light knock condition
Overall CR variation	From 5.41 to 9.18
Overall air/fuel ratio	Stoichiometric
Spark advance (SA)	10, 30 CAD BTDC
LPG mass fraction in the fuel mixture	0%, 20%, 40%, 60%, 80%

Table 3 Engine compression ratios used in the different operative conditions

		LPG mass fraction in the fuel mixture				
SA (CAD)	T_{man} (°C)	0%	20%	40%	60%	80%
10	50	7.47	8.26	8.63	8.89	8.89
	80	7.12	7.87	8.14	8.38	8.50
	110	6.92	7.47	7.77	7.87	8.03
	140	6.70	7.21	7.43	7.52	7.62
30	50	6.11	6.49	6.70	6.84	6.92
	80	5.86	6.17	6.33	6.42	6.52
	110	5.50	5.81	6.03	6.11	6.20
	140	5.41	5.64	5.74	5.84	5.95

Table 4 Properties of Euro premium gasoline and LPG

Properties	Gasoline	LPG
Composition	Commercial gasoline	75% propane, 25% propylene
Motor octane number (MON)	84	93
Lower heating value (MJ/kg)	44	46
Stoichiometric air/fuel ratio (mass)	14.7	15.5
Density at 15°C and 1 bar (kg/m^3)	735	1.85

spark ignition, the unburned gas temperature has been assumed to follow a polytropic law, hence:

$$T = T_{IGN}\left(\frac{p}{p_{IGN}}\right)^{\frac{m-1}{m}} \tag{6}$$

where T_{IGN} and p_{IGN} are the unburned gas temperature and pressure at spark ignition, while m is the polytropic coefficient, which, following the indications of Randolph (1990) and those of Brunt and Pond (1997), has been fixed to 1.32. An example of raw pressure signal power spectrum is reported in Figure 5; knocking produces pressure oscillations whose main frequency is around 6 kHz. The pressure signal has been filtered by means of a second order, zero-phase shift, band-pass 3–20 kHz Butterworth filter in order to remove unwanted noise and highlight knocking pressure oscillations. For each recorded pressure cycle the experimental knock onset crank angle (KOCA) $\vartheta_{KO\,exp.}$ has been identified as the location of the first band pass filtered pressure oscillation higher than 0.2 bar peak to peak (this threshold has been fixed based on previous experimental experience). The pressure cycles with peak to peak pressure oscillations higher than 0.6 bar have been excluded from the calibration procedure in order to obtain a model that correctly predicts early knocking. Figure 6 shows a typical light knocking pressure curve, obtained with gasoline, together with its band-pass filtered signal: the $\vartheta_{KO\,exp.}$ is highlighted. Figure 7 shows a light knocking pressure curve obtained with LPG, for the same spark advance and inlet mixture temperature of Figure 6; the maximum pressure is higher and the knock onset position is nearer TDC.

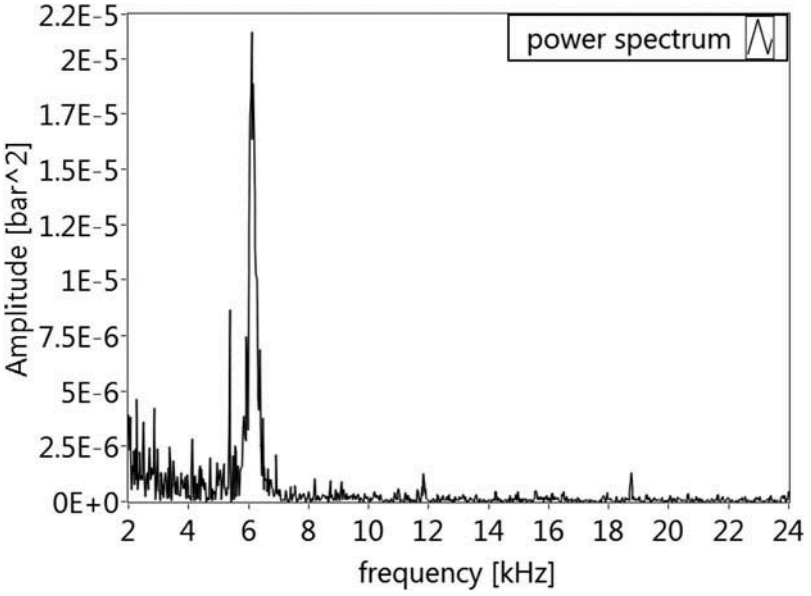

Figure 5 Power spectrum of the raw pressure signal (gasoline, SA = 30 CAD BTDC, $T_{MAN} = 140°C$).

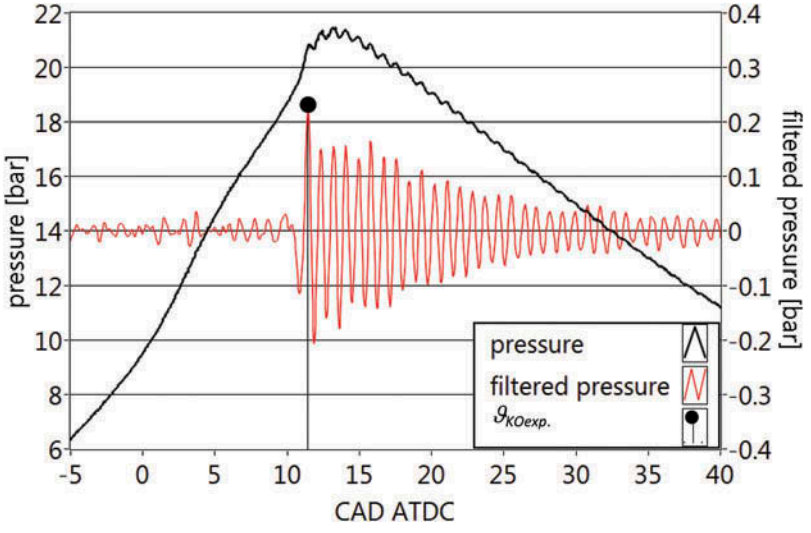

Figure 6 Raw and filtered pressure with $\vartheta_{KO\,exp.}$ evaluation (gasoline, SA = 30 CAD BTDC, $T_{MAN} = 140°C$).

Once known the $\vartheta_{KO\,exp.}$ for each of the pressure cycles sampled, the estimated KOCA $\vartheta_{KO\,est.}$ has been determined solving the knock integral of Eq. (3) in the crank angle domain as reported here:

$$\int_{\vartheta_{IVC}}^{\vartheta_{KO\ est.}} \frac{d\vartheta}{\omega \cdot A \cdot p^{-n} \cdot e^{B/T}} = 1 \tag{7}$$

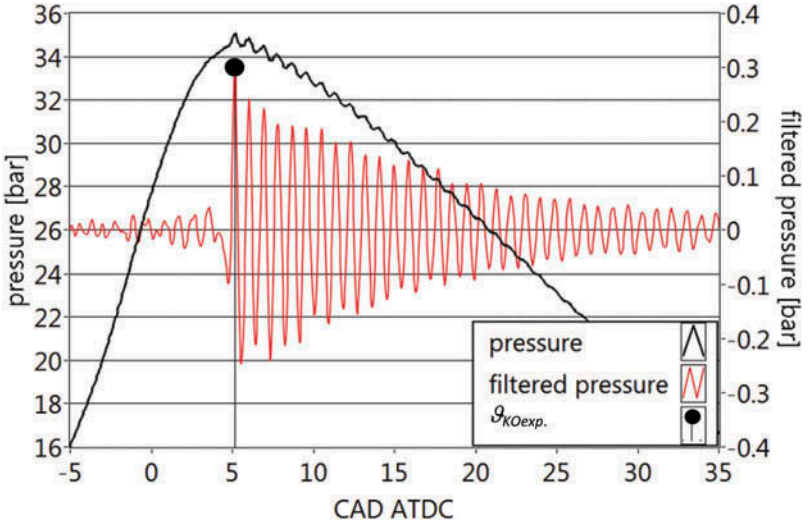

Figure 7 Raw and filtered pressure with $\vartheta_{KO\,exp.}$ evaluation (LPG, SA = 30 CAD BTDC, $T_{MAN} = 140°C$).

where ϑ_{IVC} is the IVC crank angle while ω is the engine angular velocity. The KOCA error ε can be evaluated for each fixed set of constants A, n, and B using the following equation:

$$\varepsilon = \vartheta_{KO\ est.} - \vartheta_{KO\ exp.} \tag{8}$$

The optimal set of constants A, n, and B has been determined minimizing the mean absolute error ε_{MA} evaluated over the total number of pressure cycles N:

$$\varepsilon_{MA} = \frac{\sum_{i=1}^{N} |\varepsilon_i|}{N} \tag{9}$$

For a fixed set of n and B, values the A constant has been varied, using a Downhill Simplex searching algorithm (Nelder and Mead, 1965), in order to minimize the objective function $\varepsilon_{MA}(A, B, n)$; this method has been repeated for B ranging from 1000 to 4000 and n ranging from 1.5 to 3.5.

This procedure allowed to trace the surface and the contour map of the minimum ε_{MA}, reported in Figure 8 and in Figure 9, respectively, as function of B and n: the cross, which indicates the absolute minimum of ε_{MA}, provides the values of the three model constants reported in Table 5.

The ID method (4) was also taken into consideration and compared with the integral method in terms of knock onset prediction reliability. The estimated KOCA, according to Eq. (4), is:

$$\vartheta_{KOest.ID} = \omega \cdot A p_m^{-n} e^{B/T_m} \tag{10}$$

where p_m [bar] and T_m [K] are the experimental unburned gas mean pressure and temperature (Eq. (6)), evaluated from spark ignition to knock onset. For a fixed set of model constants A, n, and B the KOCA error ε_{ID} is evaluated by Eq. (8) and the mean absolute error

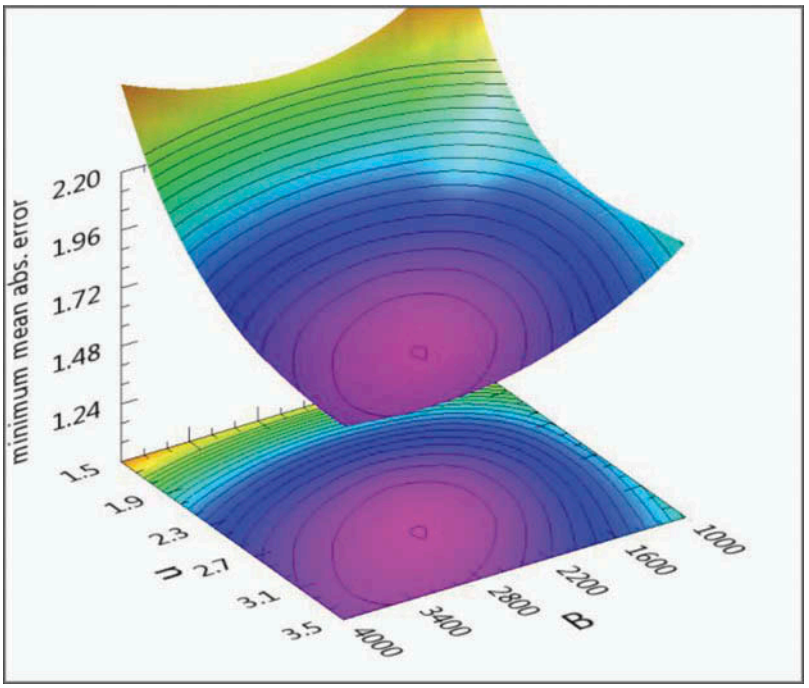

Figure 8 Surface of the minimum ε_{MA} as a function of integral model constants B and n for gasoline.

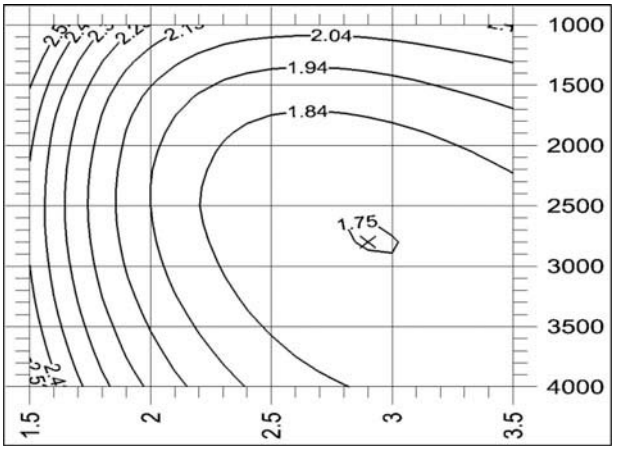

Figure 9 Contour map of the minimum ε_{MA} as a function of integral model constants B and n for gasoline.

Table 5 Values of the integral model constants obtained for gasoline

Fuel	A	n	B	ε_{MA} (CAD)	$\varepsilon_{\mathrm{MAX.}}$ (CAD)
Gasoline	0.34	2.90	2800	1.74	5.6

Table 6 Values of the ID model constants obtained for gasoline

Fuel	A	n	B	$\varepsilon_{MA\ ID}$ (CAD)	$\varepsilon_{\mathrm{MAX.}\ ID}$ (CAD)
Gasoline	0.25	2.65	2250	1.94	6.8

$\varepsilon_{MA\ ID}$ by Eq. (9). Following the minimization procedure previously described, the minimum error model constants have been determined (Table 6). Both ID and integral method provided quite similar constants with a comparable level of accuracy for what concerns $\varepsilon_{MA,ID}$.

As regards the simultaneous combustion of LPG and gasoline, some preliminary considerations have to be pointed out. As shown in previous works (Genchi et al., 2013; Pipitone and Beccari 2010; Pipitone and Genchi, 2014) the gasoline-air mixture strongly benefits from the addition of LPG in terms of knock resistance. Similar conclusions can be drawn considering the increments of knocking compression ratio due to the addition of LPG to gasoline (see Table 3). During flame front propagation, each fuel in the unburned mixture features a certain number of pre-ignition reactions, which are essentially governed by the radicals produced by each single fuel component. Gasoline composition, mainly characterized by C_4 to C_{12} hydrocarbons (as stated by American Petroleum Institute (1988) and Nikolaou et al. (2004)), is very different from that of LPG, which is a C_3 hydrocarbons mixture (Table 4), but may also contain C_4 hydrocarbons. As a consequence, the radicals involved in the chain-branching reactions of gasoline are quite different from those produced by LPG, characterized by lower reaction rate and longer lives (Kukkadapu, 2012; Prince and Williams, 2012). This explains the higher knock resistance of LPG (93 MON) with respect to gasoline (84 MON). Therefore, a possible explanation of the knocking resistance increase obtained by adding LPG to gasoline may be given by supposing that LPG intermediate products interact with gasoline radicals slowing down their reactions and hence the overall auto-ignition process (i.e., increasing the auto-ignition delay). According to the above mentioned considerations, in the simultaneous combustion of LPG and gasoline, the auto-ignition process is promoted by the lower knock resistant fuel (gasoline) and slowed down by the higher resistant (LPG). In the two auto-ignition models (Eqs. (3) and (4)), the constants n and B represent the fuel sensitivity to pressure and temperature histories. Hence, for LPG-gasoline mixtures combustion the authors used the n and B values determined for pure gasoline, ascribing only to the constant A the increased auto-ignition time due to LPG participation. The same procedure has been followed by Douaud and Eyzat (1978) for the simultaneous combustion of n-heptane and isooctane and by Pipitone and Beccari (2009b) for the combustion of CNG-gasoline mixtures. Therefore, for each LPG-gasoline mixture tested, the authors determined only the value of the A constant minimizing the mean absolute error ε_{MA} of Eq. (9); the results, obtained by means of the integral method, are reported in Table 7 with the corresponding ε_{MA} and maximum error $\varepsilon_{\mathrm{MAX}}$.

The same procedure has been followed for the ID method providing the results reported in Table 8.

The two methods provided quite similar results in terms of A constant and mean error even though the ID method features a higher maximum error $\varepsilon_{\mathrm{max.}\ ID}$, 9.6 CAD against 6.0 CAD of the integral method. Figure 10 shows the model constant A as function of LPG mass fraction; as can be observed a clear linear regression can be drawn for each method.

This means that the auto-ignition time of the double-fuel mixture linearly depends on LPG mass fraction. This is a remarkable property, since, by means of linear interpolation,

Table 7 Values of the constant *A* obtained for each LPG-gasoline mixture tested (integral method)

LPG mass fraction (%)	*A*	ε_{MA} (CAD)	$\varepsilon_{MAX.}$ (CAD)
0	0.34	1.74	5.6
20	0.40	1.81	5.9
40	0.46	1.84	5.7
60	0.53	1.86	6.0
80	0.58	1.86	5.2

Table 8 Values of the constant *A* obtained for each LPG-gasoline mixture tested (ID method)

LPG mass fraction (%)	*A*	$\varepsilon_{MA\ ID}$ (CAD)	$\varepsilon_{MAX.\ ID}$ (CAD)
0	0.25	1.94	6.80
20	0.29	2.05	8.20
40	0.33	2.08	9.00
60	0.37	2.01	9.60
80	0.40	1.96	7.50

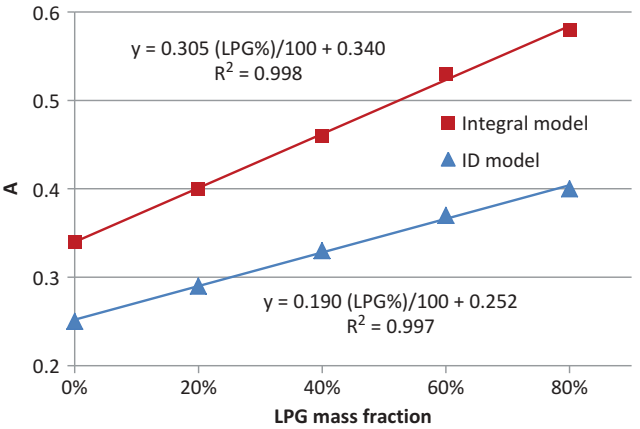

Figure 10 Models constant *A* as function of the LPG mass fraction.

it allows to determine the constant *A* of the knock prediction models for LPG mass fraction ranging from 0% to 99%. On the other hand, LPG mass fraction higher than 80% may not be useful since in a previous work Pipitone and Beccari (2010) showed that the maximum engine efficiency was reached employing LPG mass fractions between 60% and 80%. Moreover, the linear regressions in Figure 10 cannot include the 100% LPG because the diagrams are based on constants *n* and *B* determined for gasoline. A correlation between the constant *A* and the fuel mixture octane number may be very useful, as already stated by Douaud and Eyzat (1978). In a previous work, Genchi et al. (2013) determined a correlation between the LPG mass fraction and the MON of an LPG-gasoline mixture. The results are shown in Figure 11 with the polynomial curve fit; using those results it is possible to trace an experimental correlation between the constant *A* and the fuel mixture MON.

This correlation is shown in Figure 12 together with the best fit curve whose equation is:

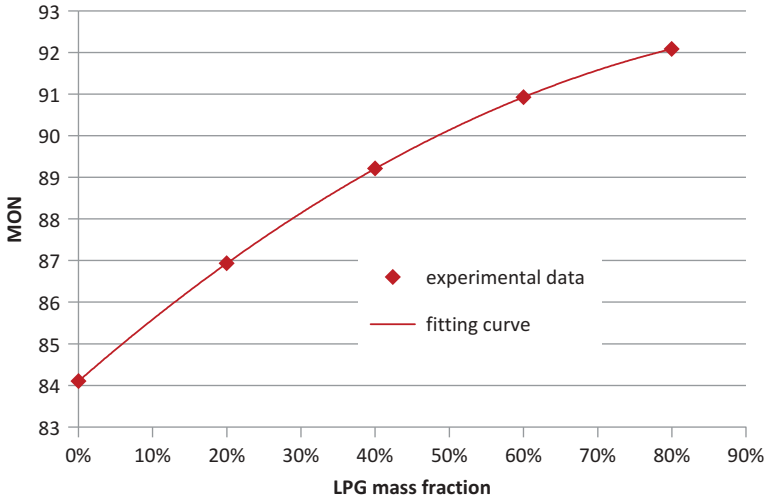

Figure 11 Fuel mixture MON as function of the LPG mass fraction.

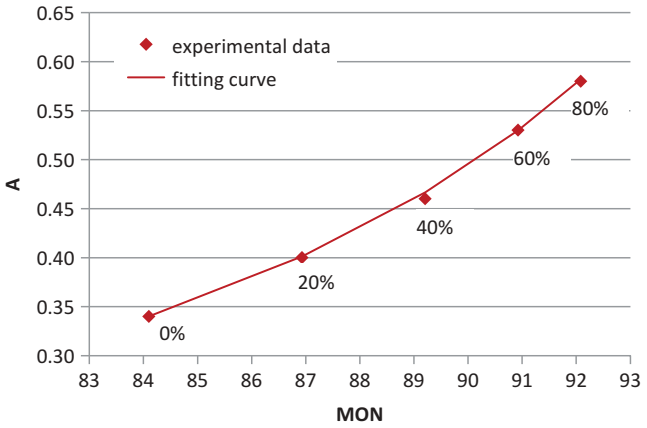

Figure 12 Model constant A as function of the mixture MON (LPG mass fraction is also reported).

$$A = (11.1 - 0.1038 \cdot \mathrm{MON})^{-1.25} \tag{11}$$

The constant A trend shows an increasing slope with mixture MON that implies a nonlinear correlation between auto-ignition time and MON.

To resume the results of all tests, for each LPG mass fraction (i.e., for each set of constants A, n, and B), the $\vartheta_{KO\,est.}$ estimated by the integral method has been compared with the corresponding $\vartheta_{KO\,exp.}$. Figure 13 reveals a good correlation between numerical and experimental data with an overall R^2 value of 0.924, a maximum difference of ± 6 CAD, and an overall mean absolute difference of 1.82 CAD. The maximum integral method error of 6 CAD is a satisfactory result considering the large variety of pressure and temperature histories used for model calibration. Furthermore, for what concerns SI engine control, Pipitone (2008) found that a spark advance error of 5 CAD, with respect to the value that

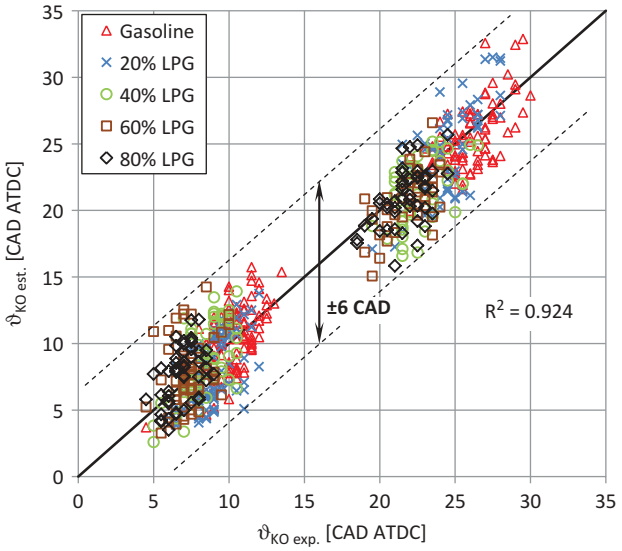

Figure 13 Comparison between estimated and experimental knock onset crank angles (integral method).

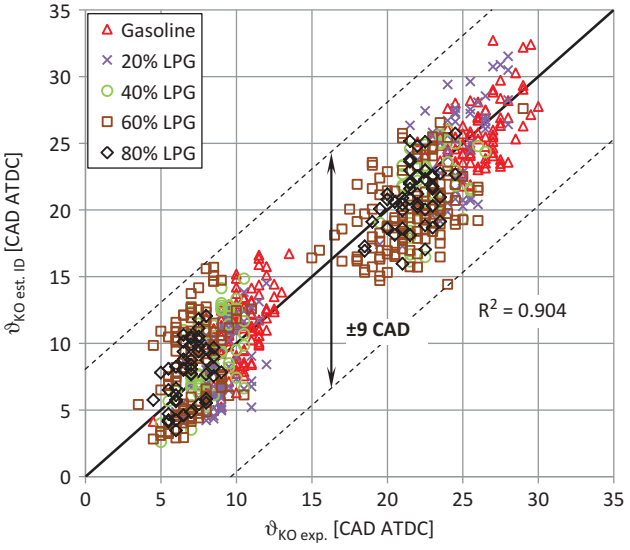

Figure 14 Comparison between estimated and experimental knock onset crank angles (ID method).

provides the maximum brake torque, leads to a 1% decrease in brake thermal efficiency. Moreover, also the most sophisticated spark advance feedback controls are affected by errors up to 4 CAD (Pipitone, 2014).

The same procedure has been followed for the ID method; the results reported in Figure 14 show an overall R^2 value of 0.904, a maximum difference of ±9 CAD, and an overall mean absolute difference of 2.01 CAD. Both models show high accuracy (i.e., a low ε_{MA}) but the ID method features a lower precision (i.e., a higher $\varepsilon_{\mathrm{MAX}}$), probably due to its

intrinsic simplicity. As a consequence, since the computational effort is almost the same for both methods, the integral model is preferred.

CONCLUSIONS

The aim of this work was to provide a reliable knock prediction sub-model to be used in engine thermodynamic simulations for a knock-safe performance optimization of engines fueled by LPG-gasoline mixtures. This has been accomplished by using two different methods, the knock-integral and the ignition delay. In the model calibration process, a heterogeneous set of experimental data has been used in order to predict knock occurrence in engines of different types (aspirated or supercharged) and with different geometries (i.e., compression ratio). The experimental results show that the auto-ignition time of the LPG-gasoline mixtures linearly depends on the LPG mass fraction and it is correlated with the mixtures MON by an increasing slope trend. The integral model allows predicting the knock onset position with a maximum error of 6 CAD and a mean absolute error of just 1.82 CAD. This is quite a satisfactory result since, from an engine control standpoint, a spark advance error of 5 CAD, with respect to the value that provides the maximum brake torque, leads to a 1% decrease in brake thermal efficiency (Pipitone, 2008). Moreover, the most sophisticated spark advance feedback controls are affected by errors up to 4 CAD (Pipitone, 2014). Finally, the integral model has been compared with the ID method, which featured lower accuracy with a maximum error of 9 CAD and a mean absolute error of 2.01 CAD. For this reason and considering that the two methods require similar computational effort, the integral model is preferable.

NOMENCLATURE

A, n, B	fuel dependent model constants
CAD	crank angle degrees
CFR	cooperative fuel research
CR	compression ratio
E	fuel activation energy
ID	ignition delay
IVC	inlet valve closure
KI	knock integral
KOCA	knock onset crank angle
LPG	liquefied petroleum gas
m	polytropic law coefficient
MAP	manifold absolute pressure
MON	motor octane number
N	total number of pressure cycles
NG	natural gas
p	unburned gas pressure
p_{IGN}	unburned gas pressure at spark ignition
p_{IVC}	unburned gas pressure at IVC
p_m	experimental unburned gas mean pressure
R	universal gas constant
SA	spark advance

SI	spark ignition
t	time
T	unburned gas temperature
TDC	top dead center
T_{IGN}	unburned gas temperature at spark ignition
t_{IVC}	inlet valve closure time
T_{IVC}	unburned gas temperature at IVC
t_{KO}	knock onset time
T_m	experimental unburned gas mean temperature
T_{MAN}	inlet mixture temperature
UEGO	universal exhaust gas oxygen
V	in-cylinder volume
V_{IVC}	unburned gas volume at IVC
ϑ_{IVC}	IVC crank angle
$\vartheta_{KO\,est.}$	KOCA estimated using the integral method
$\vartheta_{KO\,est.\,\mathrm{ID}}$	KOCA estimated using the ID method
$\vartheta_{KO\,exp.}$	experimental KOCA
ε	KOCA error
ε_{MA}	mean absolute error of the integral model
$\varepsilon_{MA\,ID}$	mean absolute error of the ID model
$\varepsilon_{\mathrm{MAX}}$	maximum error of the integral model
$\varepsilon_{\mathrm{MAX}\,ID}$	maximum error of the ID model
τ	ignition delay
ω	engine angular velocity

REFERENCES

American Petroleum Institute. 1988. *Alcohols and Ethers*, 2nd ed., Publication No. 4261, American Petroleum Institute, Washington DC.

ASTM International. 2013. Standard test method for motor octane number of spark-ignition engine fuel. ASTM D2700-13b.

Boehman, A.L., and Le Corre, O. 2008. Combustion of syngas in internal combustion engines. *Combust. Sci. Technol.*, **180**, 1193–1206.

Brunt, M., and Pond, C. 1997. Evaluation of techniques for absolute cylinder pressure correction. SAE Paper 970036.

Douaud, A.M., and Eyzat, P. 1978. Four-octane-number method for predicting the anti-knock behaviour of fuels and engines. SAE Paper 780080.

Genchi, G., Pipitone, E., Beccari, S., and Piacentino, A. 2013. Knock resistance increase through the addition of natural gas or LPG to gasoline: An experimental study. SAE Paper 2013-24-0100.

Heywood, J.B. 1988. *Internal Combustion Engines Fundamentals*, McGraw-Hill, New York.

Kukkadapu, G., Kumar, K., Sung, C.J., Mehl, M., and Pitz, W.J. 2012. Experimental and surrogate modelling study of gasoline ignition in a rapid compression machine. *Combust. Flame*, **159**(10), 3066–3078.

Lämmle, C. 2005. Numerical and experimental study of flame propagation and knock in a compressed natural gas engine. PhD thesis. Swiss Federal Institute Of Technology, Zurich, Switzerland.

Linvengood, J.C., and Wu, P.C. 1955. Correlation of auto-ignition phenomena in internal combustion engines and rapid compression machines. *Symp. (Int.) Combust.*, **5**, 347–356.

Moses, E., Yarin, A.L., and Bar-Yoseph, P. 1995. On knocking prediction in spark ignition engines. *Combust. Flame*, **101**, 239–261.

Nelder, J.A., and Mead, R. 1965. A simplex method for function minimization. *Computer J*., **7**, 308–313.

Nikolaou, N., Papadopoulos, C.E., Gaglias, I.A., and Pitarakis, K.G. 2004. A new non-linear calculation method of isomerisation gasoline research octane number based on gas chromatographic data. *Fuel*, **83**(4–5), 517–523.

Pipitone, E. 2008. A comparison between combustion phase indicators for optimal spark timing. *J. Eng. Gas Turbines Power*, **130**(5), art. 052808.

Pipitone, E. 2014. Spark ignition feedback control by means of combustion phase indicators on steady and transient operation. *J. Dyn. Syst. Meas. Contr*., **136**(5), 051021/01–051021/10.

Pipitone, E., and Beccari, S. 2009a. Performances improvement of a S.I. CNG bi-fuel engine by means of double-fuel injection. SAE Paper 2009-24-0058.

Pipitone, E., and Beccari, S. 2009b. Calibration of a knock prediction model for the combustion of gasoline-natural gas mixtures. In *Proceedings of ASME I.C.E. Division Fall Technical Conference*, Lucerne, Switzerland, September 27–30; American Society of Mechanical Engineers, New York, pp. 191–197.

Pipitone, E., and Beccari, S. 2010. Performances and emissions improvement of an S.I. engine fuelled by LPG/gasoline mixtures. SAE Paper 2010-01-0615.

Pipitone, E., Beccari, A., and Beccari, S. 2008. Reliable TDC position determination: a comparison of different thermodynamic methods through experimental data and simulations. SAE Paper 2008-36-0059.

Pipitone, E., and Genchi, G. 2014. Experimental determination of liquefied petroleum gas-gasoline mixtures knock resistance. *J. Eng. Gas Turbines Power*, **136**(12), art. 121502.

Prince, J.C., and Williams, F.A. 2012. Short chemical-kinetic mechanisms for low-temperature ignition of propane and ethane. *Combust. Flame*, **159**(7), 2336–2344.

Ramos, J.I. 1989. *Internal Combustion Engine Modeling*, Hemisphere Publishing Corp., New York.

Randolph, A. 1990. Methods of processing cylinder pressure transducer signals to maximize data accuracy. SAE Paper 900170.

Soylu, S., and Gerpen, J.V. 2003. Development of an auto-ignition sub-model for natural gas engines. *Fuel*, **82**, 1699–1707.

Wayne, W., Clark, N., and Atkinson, C. 1998. Numerical prediction of knock in a bi-fuel engine. SAE Paper 982533.

Westbrook, C.K., and Pitz, W.J. 1990. Modeling of knock in spark-ignition engines. International Symposium COMODIA 90.